

# Gating Properties of Na<sub>v</sub>1.7 and Na<sub>v</sub>1.8 Peripheral Nerve Sodium Channels

Kausalia Vijayaragavan,<sup>1,2</sup> Michael E. O'Leary,<sup>3</sup> and Mohamed Chahine<sup>1,2</sup>

<sup>1</sup>Laval University, Faculty of Medicine, Sainte-Foy, Québec, Canada G1K 7P4, <sup>2</sup>Québec Heart Institute, Laval Hospital, Research Center, Sainte-Foy, Québec, Canada G1V 4G5, and <sup>3</sup>Department of Pathology, Anatomy and Cell Biology, Thomas Jefferson Medical College, Philadelphia, Pennsylvania 19107

Several distinct components of voltage-gated sodium current have been recorded from native dorsal root ganglion (DRG) neurons that display differences in gating and pharmacology. This study compares the electrophysiological properties of two peripheral nerve sodium channels that are expressed selectively in DRG neurons (Na<sub>v</sub>1.7 and Na<sub>v</sub>1.8). Recombinant Na<sub>v</sub>1.7 and Na<sub>v</sub>1.8 sodium channels were coexpressed with the auxiliary  $\beta_1$  subunit in *Xenopus* oocytes. In this system coexpression of the  $\beta_1$  subunit with Na<sub>v</sub>1.7 and Na<sub>v</sub>1.8 channels results in more rapid inactivation, a shift in midpoints of steady-state activation and inactivation to more hyperpolarizing potentials, and an acceleration of recovery from inactivation. The coinjection of  $\beta_1$  subunit also significantly increases the expression of Na<sub>v</sub>1.8 by sixfold but has no effect on the expression of Na<sub>v</sub>1.7. In addition, a great percentage of Na<sub>v</sub>1.8+ $\beta_1$  channels

is observed to enter rapidly into the slow inactivated states, in contrast to Na<sub>v</sub>1.7+ $\beta_1$  channels. Consequently, the rapid entry into slow inactivation is believed to cause a frequency-dependent reduction of Na<sub>v</sub>1.8+ $\beta_1$  channel amplitudes, seen during repetitive pulsing between 1 and 2 Hz. However, at higher frequencies (>20 Hz) Na<sub>v</sub>1.8+ $\beta_1$  channels reach a steady state to ~42% of total current. The presence of this steady-state sodium channel activity, coupled with the high activation threshold ( $V_{0.5} = -3.3$  mV) of Na<sub>v</sub>1.8+ $\beta_1$ , could enable the nociceptive fibers to fire spontaneously after nerve injury.

**Key words:** Na<sub>v</sub>1.7; Na<sub>v</sub>1.8; peripheral nerve sodium channels; expression; dorsal root ganglion; nociception; *Xenopus* oocytes

Voltage-gated sodium channels play an important role in the generation and propagation of action potentials in excitable tissues. At least 10 distinct isoforms of the sodium channel have been identified in brain and neuronal and striated muscle that differ in primary structure, pharmacology, permeation, and gating (Goldin et al., 2000). A major determinant of the functional difference among these isoforms is inherent in the  $\alpha$  subunit that determines the selectivity and gating properties of these channels (Goldin et al., 1986). However, *in vivo*, most sodium channels are associated with auxiliary subunits ( $\beta_1$ – $\beta_3$ ) that are known to modulate gating and levels of expression (Isom et al., 1992; Morgan et al., 2000). For instance, the inactivation of rat brain sodium channels (Na<sub>v</sub>1.2) is accelerated and the gating is shifted toward more hyperpolarized voltages when coexpressed with the  $\beta_1$  subunit (O'Leary, 1998). Similar findings have been reported for the skeletal muscle sodium channels, indicating that these auxiliary subunits play an important role in determining the gating properties of these tetrodotoxin-sensitive sodium channels (Bennett et al., 1993; Wallner et al., 1993; Yang et al., 1993). In contrast, the tetrodotoxin-resistant cardiac sodium channels display only subtle changes in gating when coexpressed with the  $\beta_1$

subunit (Makita et al., 1994; Nuss et al., 1995; Makielski et al., 1996).

In addition to changes in gating, the  $\beta_1$  subunit is known to enhance the expression of many sodium channels (Chahine et al., 1994; Nuss et al., 1995). The expression of functional Na<sub>v</sub>1.2 brain sodium channels increases by 2.5-fold when coexpressed with the  $\beta_1$  subunit (Isom et al., 1992). The  $\beta_1$  subunit also is believed to contribute to clustering and remodeling of sodium channels at the neuromuscular junction (Blackburn-Munro and Fleetwood-Walker, 1999; Caldwell, 2000). Such regulations may have important consequences for neuronal tissues such as dorsal root ganglion cells (DRG) in which multiple isoforms of the sodium channels are expressed in the same cell (Akopian et al., 1996; Black et al., 1996; Sangameswaran et al., 1996, 1997; Toledo-Aral et al., 1997).

At least five distinct components of voltage-gated sodium channels have been recorded from DRG neurons (Rush et al., 1998). Two components predominate in the small nociceptive neurons: a rapidly inactivating TTX-S current and a slowly inactivating TTX-R current (Kostyuk et al., 1981; Roy and Narahashi, 1992; Elliott and Elliott, 1993; Black et al., 1996). Recently, two peripheral nerve sodium channels have been isolated from the human and rat DRG (Sangameswaran et al., 1996; Toledo-Aral et al., 1997). Na<sub>v</sub>1.7 (PN1) is a TTX-S rapidly inactivating channel that is expressed widely in DRG neurons (Sangameswaran et al., 1997; Toledo-Aral et al., 1997). Na<sub>v</sub>1.8 (PN3) is a TTX-R slowly inactivating channel that is expressed predominantly in the small nociceptive C-type pain fibers (Akopian et al., 1996; Sangameswaran et al., 1996). Recently, a novel sodium channel Na<sub>v</sub>1.9 (NaN) was cloned and also may contribute to the TTX-R

Received June 1, 2001; revised July 12, 2001; accepted July 27, 2001.

This study was supported by Grant MOP-49502 from the Canadian Institutes of Health Research (CIHR) and by National Institute of General Medical Sciences Grant GM58058. M.C. is an Edwards Senior Investigator (Joseph C. Edwards Foundation), and K.V. is a recipient of a doctoral research award of the CIHR. We thank Dr. Richard Horn and Dr. Yasushi Okamura for their comments on this manuscript and Dr. G. Mandel for providing the Na<sub>v</sub>1.7 construct.

Correspondence should be addressed to Dr. M. Chahine, Laval Hospital Research Center, 2725 Chemin Sainte-Foy, Sainte-Foy, Québec, Canada G1V 4G5. E-mail: mohamed.chahine@phc.ulaval.ca.

Copyright © 2001 Society for Neuroscience 0270-6474/01/217909-10\$15.00/0

current of small DRG neurons (Dib-Hajj et al., 1998). Differential expression of the  $\text{Na}_v1.7$ ,  $\text{Na}_v1.8$ ,  $\text{Na}_v1.9$ , and several of the brain sodium channels ( $\text{Na}_v1.1$ ,  $\text{Na}_v1.2$ ,  $\text{Na}_v1.3$ ) contributes to the unique electrical excitability of nociceptive neurons (Porreca et al., 1999). Changes in the expression levels of these channels have been implicated in the alterations of neuronal excitability associated with acute and chronic pain syndromes (Rizzo et al., 1995; Gold et al., 1996).

The transcript encoding for the  $\beta_1$  subunit is present in both large and small DRG neurons (Oh et al., 1995; Coward et al., 2001). However, previous studies indicate that the  $\beta_1$  subunit does not alter the gating of  $\text{Na}_v1.7$  and  $\text{Na}_v1.8$  sodium channels (Sangameswaran et al., 1996, 1997). This finding is inconsistent with studies showing that many, if not all, sodium channels are modulated by the  $\beta_1$  subunit (Chahine et al., 1994; Isom et al., 1995). In addition, a recent study has shown that the inactivation of heterologously expressed  $\text{Na}_v1.7$  channels is accelerated when coexpressed with the  $\beta_1$  subunit (Shcherbatko et al., 1999). Currently, little is known about the modulatory effects of the  $\beta_1$  subunit on  $\text{Na}_v1.8$  channels. In this study the  $\alpha$  subunits of  $\text{Na}_v1.7$  and  $\text{Na}_v1.8$  sodium channels were expressed in *Xenopus* oocytes, and the kinetics and voltage sensitivity were compared with and without the coexpressed  $\beta_1$  subunit. The *Xenopus* oocyte system of expression was used in this study especially because the  $\text{Na}_v1.8$  sodium channels expressed, with or without the  $\beta_1$  subunit, poorly in the mammalian cell systems (tsA201 and CHO cell line). Coexpression of  $\text{Na}_v1.7$  with the  $\beta_1$  subunit in *Xenopus* oocytes causes a hyperpolarizing shift in gating and increases the rates of inactivation and recovery from inactivation. For  $\text{Na}_v1.8$  channels the  $\beta_1$  subunit produces similar changes in the voltage sensitivity and kinetics of gating but, in addition, significantly increases the expression levels of these channels. The  $\beta_1$  subunit modulates the gating of both the  $\text{Na}_v1.7$  and  $\text{Na}_v1.8$  sodium channels. Differences in the gating and expression of these sodium channels are likely to have important consequences for the generation and propagation of action potentials in nociceptive neurons.

## MATERIALS AND METHODS

**Molecular biology: Construction of full-length rat  $\alpha$  subunit  $\text{Na}_v1.8$  cDNA.** Total RNA was isolated from Sprague Dawley rat DRG by using the Trizol reagent (Life Technologies, Burlington, Ontario, Canada). Rat DRG RNA was reverse transcribed (RT) with the use of Superscript (Life Technologies) and random primers to create a cDNA library. Total DRG RNA (5  $\mu\text{g}$ ) was heat denatured at 70°C for 10 min, followed by rapid cooling on ice. Reverse transcription was performed with 10 mM deoxynucleotide triphosphate (dNTPs), 0.1 M dithiothreitol, and 50 ng/ $\mu\text{l}$  random primers in a total volume of 20  $\mu\text{l}$ . The mixture was added to the denatured total RNA and incubated at 25°C for 5 min. Superscript (1 U; Life Technologies) was added, and the reactions were incubated at 25°C for 10 min and then at 42°C for 1 hr. Incubating the sample at 70°C for 15 min then terminated the reaction. Finally, the sample was incubated at 37°C with RNaseH for 20 min to remove the total RNA. The RT product was used directly for PCR.

Rat  $\text{Na}_v1.8$   $\alpha$  subunit-specific primers were designed to amplify 2–4 kb segments within the coding region of the gene. Primer sequences were based on the published sequence (ACC number U53833). The rat  $\text{Na}_v1.8$   $\alpha$  subunit gene was amplified from the first ATG start codon; the 5' untranslated region (UTR) sequence was not included in the clone.

Primer set 1 (1–4247 bp) consisted of the following: primer position 1, sense, GAAGAATGAGAAGATGGAGCTCCCC; primer position 4247, antisense, GAGATTCAGCGTGAAGAAGCCACC. Primer set 2 (3875–5940 bp) consisted of the following: primer position 3875, sense, GTCCTCCTCGTCTGCCTCATCTTC; primer position 5940, antisense, GCCTGAGTGCCTTCACTGAGGTCCAG.

PCR was performed in a 50  $\mu\text{l}$  reaction mixture containing PCR buffer, 10 mM dNTPs, 100 ng/ $\mu\text{l}$  of the specific set of primers, 2  $\mu\text{l}$  of the rat DRG cDNA, and 1 U of Pfu-turbo Polymerase (Stratagene, La Jolla,

CA). Amplification was performed with the following cycling: 3 min at 94°C, 1 min at 94°C, 1 min at 60°C, and then 2 min/kb at 55°C repeated for a total of 30 cycles. PCR amplicons were subcloned, and the full-length  $\text{Na}_v1.8$  was constructed in the pCRII-Topo vector (Life Technologies). Full-length  $\text{Na}_v1.8$  coding sequence was confirmed by fluorescent dideoxy terminator sequencing at the automated sequencing facility of Laval University, Sainte-Foy, Québec. The final  $\text{Na}_v1.8$  construct was subcloned into pSP64T ( $\beta$ -globin), suitable for high-yield transcription of complementary RNA (cRNA).

The rat  $\text{Na}_v1.7$   $\alpha$  subunit voltage-gated sodium channel, cloned into the pCDNA3a vector, was kindly donated by Gail Mandel (Department of Neurobiology, State University of New York, NY). cRNA was prepared by the T7 (pCDNA3a) or SP6 (pSP64T) mMessage mMachine kit (Ambion, TX).

**Expression and electrophysiology in *Xenopus* oocytes.** *Xenopus laevis* females were anesthetized with 1.5 mg/ml tricaine (Sigma, Oakville, Ontario, Canada), and two or three ovarian lobes were removed surgically. Follicular cells surrounding the oocytes were removed by incubation at 22°C for 2.5 hr in calcium-free oocyte medium [containing (in mM) 82.5 NaCl, 2.5 KCl, 1  $\text{MgCl}_2$ , and 5 HEPES, pH 7.6] containing 2 mg/ml collagenase (Sigma). The oocytes were washed first in calcium-free medium and then with a 50% Leibovitz's L-15 medium (Life Technologies) enriched with 15 mM HEPES and 5 mM L-glutamine, supplemented with 10 mg/ml gentamycin, pH 7.6. The oocytes were stored in this medium until further use. Stage VI–V oocytes were selected and microinjected with 50 nl of cRNA encoding for the  $\alpha$  subunit of  $\text{Na}_v1.7$  or  $\text{Na}_v1.8$ . The amounts of  $\text{Na}_v1.7$  cRNA injected in the oocytes were lesser compared with the amounts injected for  $\text{Na}_v1.8$  channels. This is because the  $\text{Na}_v1.7$  channels express more readily compared with  $\text{Na}_v1.8$  channels. Sets of oocytes also were coinjected in parallel with equal ratios of  $\text{Na}_v1.7$  and  $\beta_1$  subunit or  $\text{Na}_v1.8$   $\alpha$  subunit and  $\beta_1$  subunit.

Oocytes were stored at 18°C and used for experiments depending on the level of expression of each channel type. Parallel sets of experiments with the rat skeletal muscle sodium channel ( $\mu 1$ ) were used to confirm the functional association of the  $\alpha$  and  $\beta_1$  subunits in oocytes (data not shown).

The whole-cell sodium current from cRNA-injected oocytes was measured via two-microelectrode voltage clamp at room temperature  $\approx 22^\circ\text{C}$ . The oocytes were impaled with  $<2$  M $\Omega$  electrodes containing 3 M KCl and were voltage clamped with an OC-725 oocyte clamp (Warner Instruments, Hamden, CT). The bath Ringer's solution contained (in mM) 90 NaCl, 2 KCl, 1.8  $\text{CaCl}_2$ , 2  $\text{MgCl}_2$ , and 5 HEPES, pH 7.6. Currents were filtered at 1.5 kHz with an eight-pole Bessel filter and were sampled at 10 kHz. Data were acquired and analyzed with pClamp software v7 (Axon Instruments, Foster City, CA).

The voltage dependence of activation was determined by eliciting depolarizing pulses from a holding potential of  $-100$  mV to potentials ranging from  $-80$  to  $+60$  mV in 10 mV increments. Current activation curves of the channels were plotted via the following Boltzmann equation:  $G_{\text{Na}}/G_{\text{Na max}} = 1/(1 + \exp((V + V_{0.5})/k))$ , for which the  $G_{\text{Na}}$  (conductance) values for each clamped oocyte were determined by dividing the peak sodium current by the driving force ( $V_m - E_{\text{Na}}$ ). The reversal potential ( $E_{\text{Na}}$ ) for each oocyte expressing the channels was estimated by extrapolating the linear ascending segment of decay gradient, between 0 and  $+20$  mV for  $\text{Na}_v1.7$  and between  $+20$  and  $+40$  mV for  $\text{Na}_v1.8$ , of an  $I$ - $V$  curve to the voltage axis.  $V$  is equal to the test voltage,  $V_{0.5}$  is the voltage at which the channels are half-maximally activated, and  $k$  is the slope factor. Conductance versus voltage data were fit with a two-state Boltzmann equation.

**Statistical analysis.** Results of representative measures were expressed by means  $\pm$  SEM. The currents of paired groups of oocytes injected with the  $\alpha$  subunit of  $\text{Na}_v1.7$  or  $\text{Na}_v1.8$  were compared directly with those of oocytes coinjected with the  $\alpha$  and  $\beta_1$  subunits; a repeated measurement ANOVA was performed. The homogeneity of correlation between repeated measures was tested with the sphericity test. The results were considered significant if  $p$  values were  $\leq 0.05$ . The data were analyzed by the statistical package program SAS (SAS Institute, Cary, NC).

## RESULTS

### Effects of $\beta_1$ subunit on the expression of $\text{Na}_v1.7$ and $\text{Na}_v1.8$ sodium channels

The  $\alpha$  subunit of the peripheral nerve sodium channel  $\text{Na}_v1.8$  was cloned from the DRG of Sprague Dawley rats via RT-PCR (see Materials and Methods). The fidelity of the  $\text{Na}_v1.8$  clone was

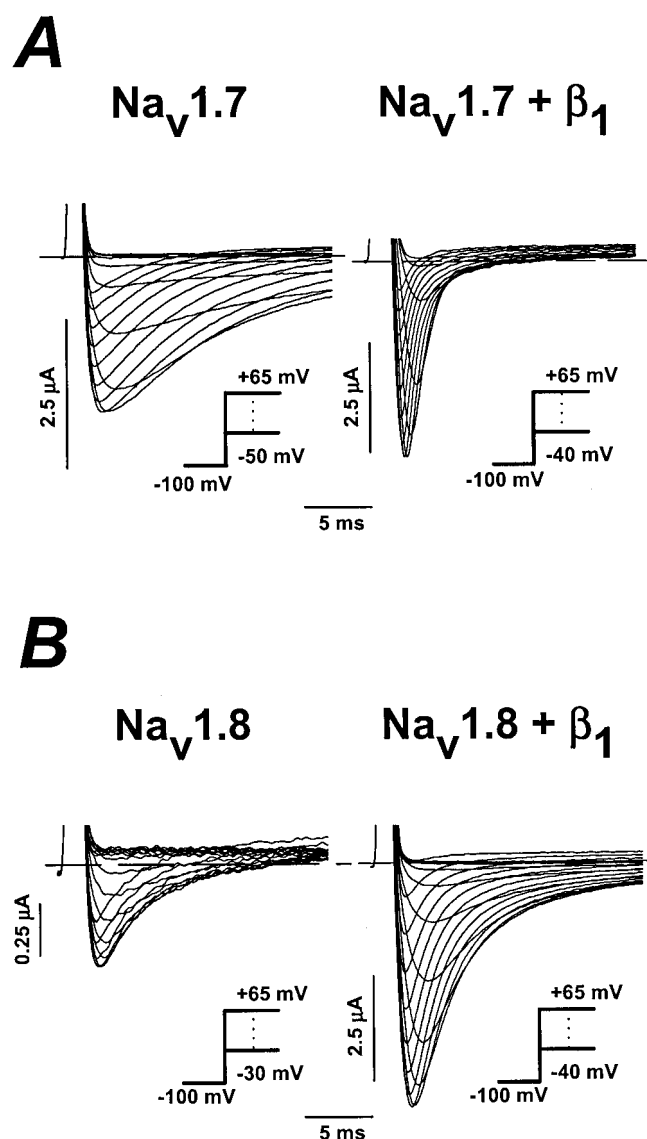


**Figure 1.** Effects of the  $\beta_1$  subunit on  $\text{Na}_v1.7$  and  $\text{Na}_v1.8$  sodium channels heterologously expressed in *Xenopus* oocytes. The data show the whole-cell sodium currents of oocytes expressing either the  $\text{Na}_v1.7$  or  $\text{Na}_v1.8$  sodium channel with and without the  $\beta_1$  subunit. Currents were elicited by depolarizing steps between  $-50$  and  $+65$  mV in  $5$  mV increments from a holding potential of  $-100$  mV (see inset). **A**, Whole-cell  $\text{Na}_v1.7$  currents measured in the absence (left) and presence (right) of the  $\beta_1$  subunit. **B**,  $\text{Na}_v1.8$  sodium currents expressed without (left) and with (right) the  $\beta_1$  subunit. Dashed lines are the zero current levels.

verified by comparing its sequence with the published sequence (ACC number U53833). cRNA of  $\text{Na}_v1.7$  and  $\text{Na}_v1.8$  clones was microinjected into stage IV–V *Xenopus* oocytes. The whole-cell sodium currents of oocytes injected with  $\text{Na}_v1.7$  and  $\text{Na}_v1.8$  channels were compared with and without the  $\beta_1$  subunit. The currents were evoked by applying a series of depolarizing voltage steps between  $-50$  and  $+65$  mV in  $5$  mV increments (Fig. 1).  $\text{Na}_v1.7$  and  $\text{Na}_v1.8$  channels have distinct expression behaviors in the *Xenopus* oocytes. The  $\text{Na}_v1.7$  currents activate at  $-40$  mV and peak at  $-20$  mV, whereas  $\text{Na}_v1.8$  currents activate and peak at  $-15$  and  $+20$  mV, respectively. For voltage pulses to  $-20$  mV, oocytes expressing the  $\text{Na}_v1.7$  channels displayed large sodium currents ( $-3087.8 \pm 435.4$  nA,  $n = 6$ ) after  $<24$  hr of incubation (Figs. 1A, 2A). In contrast, oocytes injected with  $\text{Na}_v1.8$  ex-

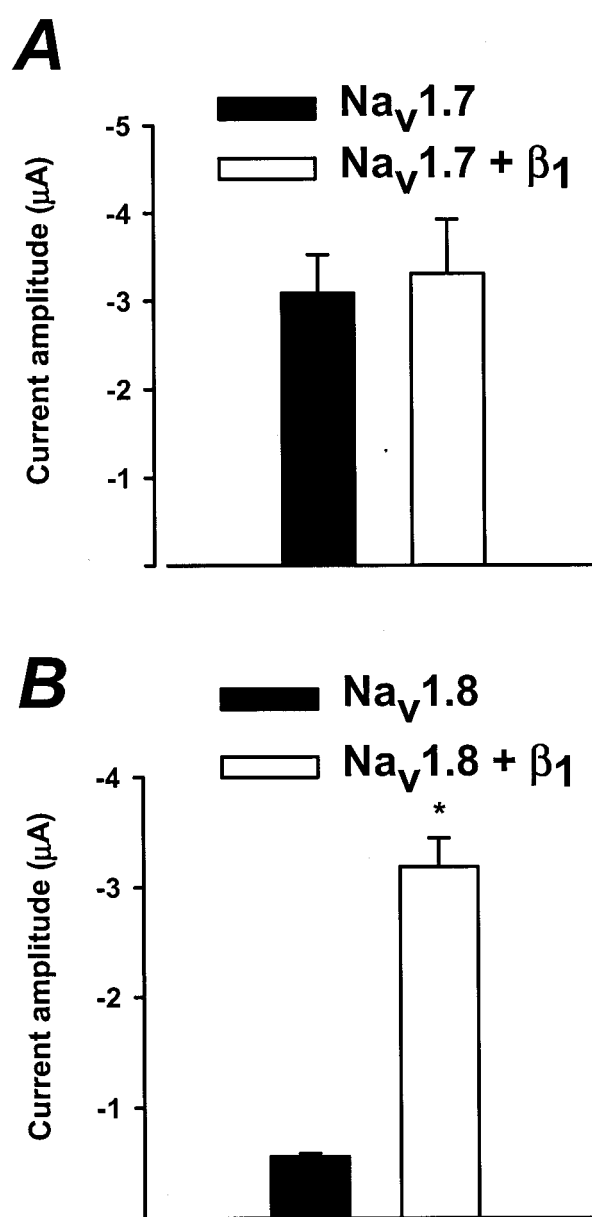


**Figure 2.** Effects of the  $\beta_1$  subunit on the expression of  $\text{Na}_v1.7$  and  $\text{Na}_v1.8$  sodium channels. Shown are the whole-cell sodium currents of paired groups of oocytes expressing either the  $\text{Na}_v1.7$  or  $\text{Na}_v1.8$  channels with or without the  $\beta_1$  subunit.  $\text{Na}_v1.7$  peak currents at  $-20$  mV were measured from oocytes expressing  $\text{Na}_v1.7$  or  $\text{Na}_v1.7 + \beta_1$  after 24 hr of incubation. There was no significant difference in the peak amplitude of current between  $\text{Na}_v1.7$  and  $\text{Na}_v1.7 + \beta_1$  even at 3 d after injection (data not shown). For  $\text{Na}_v1.8$  channels the peak currents measured at  $+20$  mV were compared 6 d after cRNA injection. Peak amplitude recorded 3 d after injection for  $\text{Nav}1.8$  channels was small ( $38.1 \pm 2.8$  nA;  $n = 3$ ), whereas the coexpression increased expression by 17-fold ( $695 \pm 117$  nA;  $n = 5$ ; data not shown). The  $\beta_1$  subunit significantly increased ( $p < 0.05$ ) the currents of  $\text{Na}_v1.8$  ( $n = 7$ ), but not the  $\text{Na}_v1.7$  ( $n = 6$ ), sodium channels ( $p < 0.05$ ). The holding potential was  $-100$  mV.

pressed small currents at  $+20$  mV ( $-557.8 \pm 26.3$  nA) after  $>5$  d after injection (Figs. 1B, 2B), indicating that the  $\alpha$  subunit of  $\text{Na}_v1.8$  is expressed inefficiently in oocytes.

Figure 2 directly compares the currents of paired groups of oocytes expressing either  $\text{Na}_v1.7$  or  $\text{Na}_v1.8$  with and without the  $\beta_1$  subunit. The sodium current of oocytes injected with  $\text{Na}_v1.8$  substantially increases when coexpressed with the  $\beta_1$  subunit (Fig.

2B). At +20 mV, coexpression with the  $\beta_1$  subunit increases the sodium current of oocytes expressing  $\text{Na}_v1.8$  by 5.7-fold ( $-3183 \pm 262$  nA) (Fig. 2B). Although the mechanism underlying this increase in current is not known, these data are similar to those of previous studies showing that the  $\beta_1$  subunit increases the expression of a number of sodium channel isoforms (Nuss et al., 1995). In contrast, the amplitude of currents of oocytes expressing  $\text{Na}_v1.7$  is not altered by the  $\beta_1$  subunit (Fig. 2A). The  $\beta_1$  subunit selectively enhances the expression of the  $\text{Na}_v1.8$  sodium channels. Both  $\text{Na}_v1.7$  and  $\text{Na}_v1.8$  sodium channels cDNAs also were transfected into different mammalian cell expression systems (tsA201 and CHO) in the absence and presence of the  $\beta_1$  subunit. However, mammalian cells transfected with  $\text{Na}_v1.8$  channels, in the absence or presence of the  $\beta_1$  subunit, expressed small to negligible amounts of current ( $\leq 1$  nA,  $n = 6$ ; data not shown). In contrast, tsA201 cells transfected with  $\text{Na}_v1.7$  cDNA expressed  $\sim 10$  nA of current ( $n = 4$ ; data not shown). Because of the poor expression of  $\text{Na}_v1.8$  channels in the different mammalian systems, *Xenopus* oocytes were used preferentially in this study.

### Effects of the $\beta_1$ subunit on kinetics of current decay of $\text{Na}_v1.7$ and $\text{Na}_v1.8$ channels

In addition to changes in expression levels, the  $\beta_1$  subunit also alters the gating properties of these channels. In the absence of the  $\beta_1$  subunit, the inactivation of  $\text{Na}_v1.7$  is slow, resulting in considerable residual current near the end of the 20 msec depolarizing pulse (Figs. 1A, 3A). When coexpressed with the  $\beta_1$  subunit, the inactivation is more rapid and the currents are inactivated completely during the 20 msec depolarization (Figs. 1A, 3A). The  $\beta_1$  subunit also accelerates the inactivation of  $\text{Na}_v1.8$  but to a much lesser extent than that observed for  $\text{Na}_v1.7$  (Fig. 3B). To quantitate the changes in decay rate, we fit the currents with single exponentials. At  $-20$  mV the decay of  $\text{Na}_v1.7$  currents has a time constant ( $\tau_h$ ) of  $19.8 \pm 3.6$  msec ( $n = 6$ ) and  $1.8 \pm 0.2$  msec ( $n = 6$ ) for  $\text{Na}_v1.7 + \beta_1$ . Coexpression with the  $\beta_1$  subunit significantly accelerates the inactivation of  $\text{Na}_v1.7$  current ( $p < 0.05$ ). Coexpression of  $\text{Na}_v1.8$  with the  $\beta_1$  subunit also significantly reduces  $\tau_h$  ( $p < 0.05$ ). At +20 mV,  $\text{Na}_v1.8$  and  $\text{Na}_v1.8 + \beta_1$  currents decay with time constants of  $4.3 \pm 0.2$  msec ( $n = 6$ ) versus  $2.6 \pm 0.1$  msec ( $n = 6$ ), respectively (Fig. 3B). The  $\beta_1$  subunit reduces the  $\tau_h$  of  $\text{Na}_v1.7$  and  $\text{Na}_v1.8$  sodium currents over a wide range of voltages (Fig. 4A,B). Overall, the data indicate that coexpression with the  $\beta_1$  subunit accelerates the inactivation of both  $\text{Na}_v1.7$  and  $\text{Na}_v1.8$  sodium channels.

### Effects of the $\beta_1$ subunit on the gating of $\text{Na}_v1.7$ and $\text{Na}_v1.8$ channels

The effect of the  $\beta_1$  subunit on the voltage sensitivity of activation was investigated also. The relative conductance was determined from families of sodium currents similar to those shown in Figure 1 (see Materials and Methods). The normalized conductance of  $\text{Na}_v1.7$  and  $\text{Na}_v1.8$  channels with and without the  $\beta_1$  subunit was plotted versus voltage (Fig. 5A,B). The smooth curves are fits to a Boltzmann function with midpoints ( $V_{0.5}$ ) and slope factors ( $k$ ) of  $-22.4 \pm 2.7$  and  $5.4 \pm 0.4$  mV ( $n = 10$ ) for  $\text{Na}_v1.7$  and of  $-27.7 \pm 1.3$  mV ( $V_{0.5}$ ) and  $3.7 \pm 0.2$  mV ( $k$ ;  $n = 11$ ) for  $\text{Na}_v1.7 + \beta_1$  (Fig. 5A). Coexpression with the  $\beta_1$  subunit causes a significant  $-5.3$  mV shift in the midpoint of steady-state activation ( $p < 0.05$ ). For  $\text{Na}_v1.8$  the  $V_{0.5}$  and  $k$  values are  $4.7 \pm 0.7$  and  $6.8 \pm 0.1$  mV ( $n = 8$ ) and  $-3.3 \pm 0.9$  mV ( $V_{0.5}$ ) and  $5.5 \pm 0.1$  mV ( $k$ ) for  $\text{Na}_v1.8 + \beta_1$  ( $n = 9$ ) (Fig. 5B). The coexpression with the  $\beta_1$  subunit causes a significant  $-8$  mV shift in midpoint ( $p < 0.05$ )

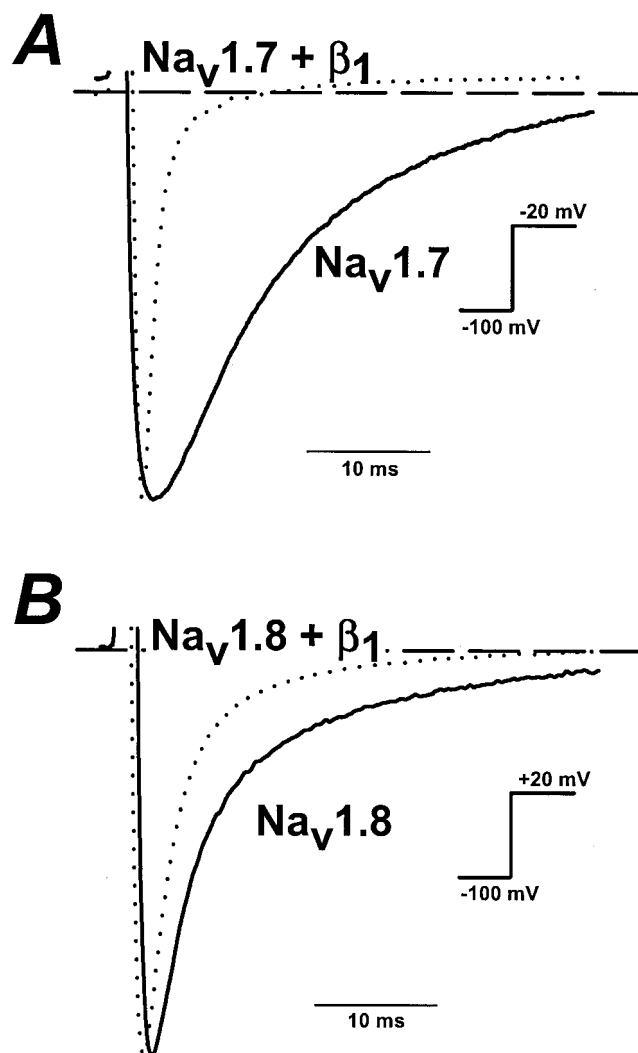


**Figure 3.** Effects of the  $\beta_1$  subunit on the kinetics of  $\text{Na}_v1.7$  and  $\text{Na}_v1.8$  inactivation. Whole-cell sodium currents of  $\text{Na}_v1.7$  and  $\text{Na}_v1.7 + \beta_1$  sodium channels were elicited by a depolarizing step from  $-100$  to  $-20$  or  $+20$  mV. Currents were normalized to facilitate comparison of the kinetics. **A**, At  $-20$  mV the time constants of current decay were  $19.8 \pm 3.6$  msec ( $n = 6$ ) and  $1.8 \pm 0.2$  msec ( $n = 6$ ) for  $\text{Na}_v1.7$  and  $\text{Na}_v1.7 + \beta_1$ , respectively. **B**,  $\text{Na}_v1.8$  and  $\text{Na}_v1.8 + \beta_1$  currents were elicited by a step depolarization to  $+20$  mV and had decay time constants of  $4.3 \pm 0.2$  msec ( $n = 6$ ) and  $2.6 \pm 0.1$  msec ( $n = 6$ ), respectively. Dashed lines are the zero current levels.

and reduces the slope factor, consistent with an increase in the voltage sensitivity of the  $\text{Na}_v1.8$  sodium channels. Overall, the  $\beta_1$  subunit causes hyperpolarizing shifts in the midpoints of activation and increases the voltage sensitivity of both  $\text{Na}_v1.7$  and  $\text{Na}_v1.8$  channels.

The effect of the  $\beta_1$  subunit on the steady-state inactivation was investigated also. Steady-state inactivation was measured by using 500 msec conditioning pulses to voltages between  $-110$  and  $+30$  mV. The fraction of available current was determined by using standard test pulses, and the normalized currents were plotted versus the conditioning voltage (Fig. 5A,B). The smooth curves are Boltzmann fits with midpoints ( $V_{0.5}$ ) and slope factors ( $k$ ) of  $-68.2 \pm 0.4$  and  $6.4 \pm 0.5$  mV ( $n = 4$ ) for  $\text{Na}_v1.7$  and of  $-69.8 \pm 0.3$  mV ( $V_{0.5}$ ) and  $3.9 \pm 0.2$  mV ( $k$ ;  $n = 4$ ) for  $\text{Na}_v1.7 + \beta_1$  (Fig. 5A). The  $\beta_1$  subunit only slightly alters the midpoint but signifi-

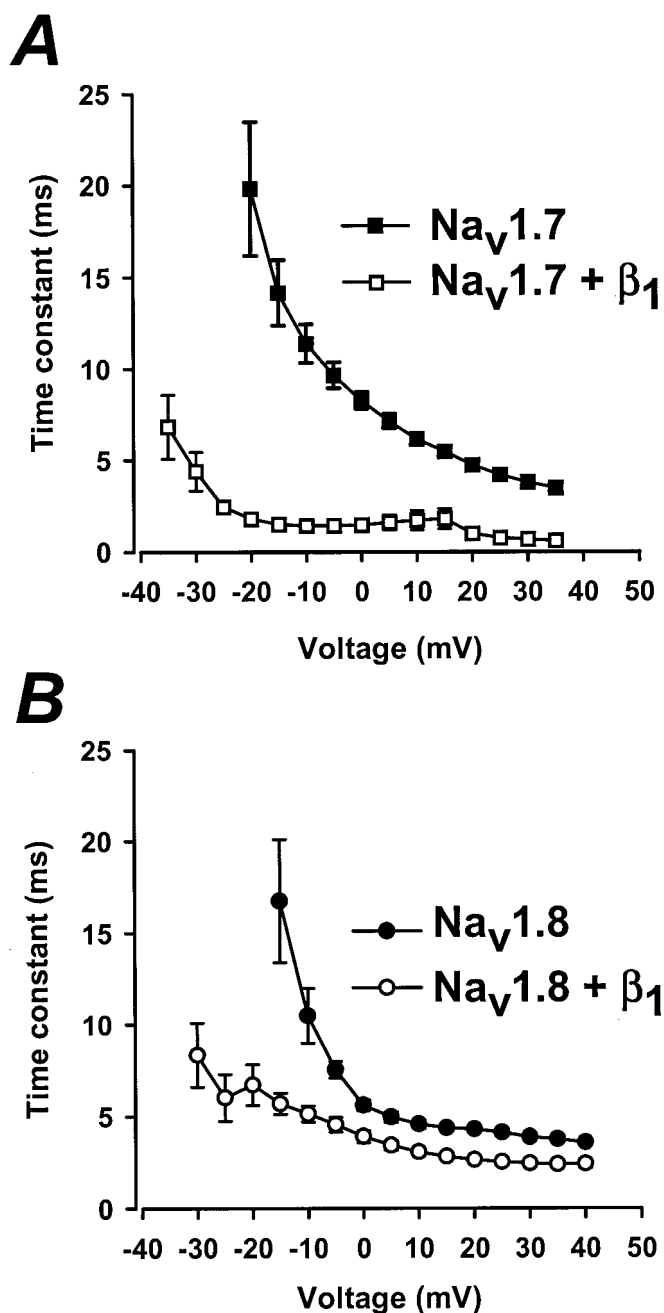


**Figure 4.** The  $\beta_1$  subunit accelerates the inactivation of  $\text{Na}_v1.7$  and  $\text{Na}_v1.8$  channels. The decay of the  $\text{Na}_v1.7$  and  $\text{Na}_v1.8$  sodium currents (Fig. 1) was fit to an exponential function, and the time constants were plotted versus the test voltage:  $I = A_1 \cdot \exp(-t/\tau) + C$ , where  $I$  is the current,  $A_1$  is the percentage of channels inactivating with time constant  $\tau$ ,  $t$  is time, and  $C$  is the steady-state asymptote. The data are the means  $\pm$  SEM of  $n = 6$  for  $\text{Na}_v1.7$  and  $\text{Na}_v1.7 + \beta_1$  and  $n = 6$  for  $\text{Na}_v1.8$  and  $\text{Na}_v1.8 + \beta_1$  channels. *A*, The inactivation time constants of  $\text{Na}_v1.7$  (filled squares) and  $\text{Na}_v1.7 + \beta_1$  (open squares) plotted versus voltage. *B*, The time constants of  $\text{Na}_v1.8$  (filled circles) and  $\text{Na}_v1.8 + \beta_1$  (open circles) plotted versus voltage.

cantly increases the voltage sensitivity of  $\text{Na}_v1.7$  inactivation ( $p < 0.05$ ). Steady-state inactivation of  $\text{Na}_v1.8$  sodium channels is shifted significantly toward hyperpolarizing voltages, with  $V_{0.5}$  and  $k$  values of  $-54.8 \pm 1.7$  and  $8.5 \pm 0.2$  mV ( $n = 3$ ) for  $\text{Na}_v1.8$  ( $p < 0.05$ ) and  $-62.6 \pm 2.3$  mV ( $V_{0.5}$ ) and  $6.3 \pm 0.7$  mV ( $k$ ;  $n = 6$ ) for  $\text{Na}_v1.8 + \beta_1$  (Fig. 5*B*). Coexpression of  $\text{Na}_v1.8$  with the  $\beta_1$

subunit significantly shifts the midpoint of steady-state inactivation by  $-7.8$  mV and increases the voltage sensitivity. Hence coexpression with the  $\beta_1$  subunit also causes hyperpolarizing shifts in the midpoints and increases the voltage sensitivity of steady-state inactivation of both the  $\text{Na}_v1.7$  and  $\text{Na}_v1.8$  sodium channels.

#### Effects of $\beta_1$ subunit on recovery from fast inactivation

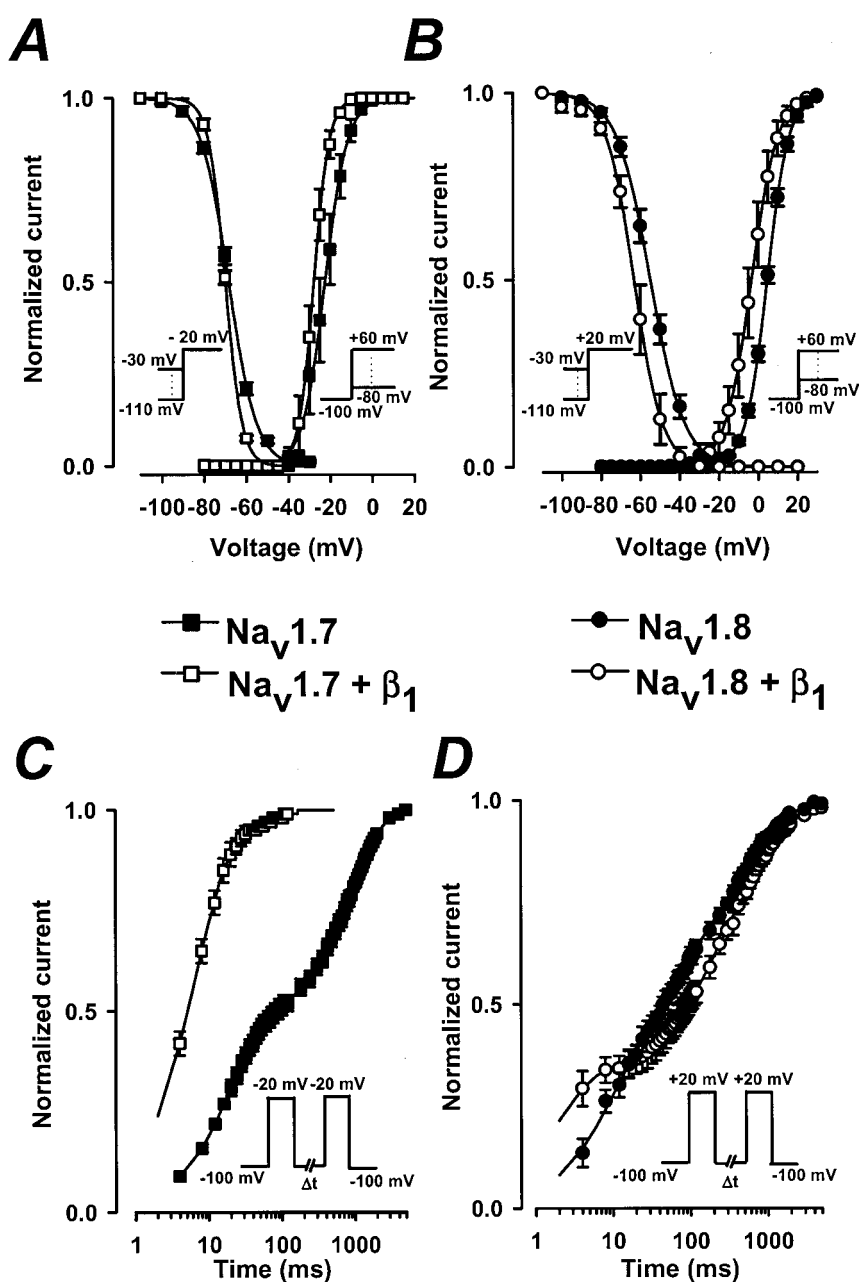
Effects of the  $\beta_1$  subunit on the recovery from fast inactivation were examined with a standard two-pulse protocol consisting of a depolarizing pulse to  $-20$  mV ( $\text{Na}_v1.7$ ) or  $+20$  mV ( $\text{Na}_v1.8$ ) for 40 msec to inactivate the channels, followed by a variable duration (1 msec to 5 sec) step to  $-100$  mV to promote recovery. The availability of the channels after the end of the recovery interval was assessed with a standard test pulse, and the normalized currents were plotted versus the recovery interval. Figure 5, *C* and *D*, illustrates the time dependence of recovery from fast inactivation of  $\text{Na}_v1.7$  and  $\text{Na}_v1.8$  channels. In the absence of the  $\beta_1$  subunit the recovery of  $\text{Na}_v1.7$  is bi-exponential, with fast and slow time constants of  $19.6 \pm 0.8$  msec ( $\tau_F$ ) and  $933.4 \pm 54.6$  msec ( $\tau_S$ ;  $n = 7$ ) (Fig. 5*C*). Coexpression with the  $\beta_1$  subunit substantially increases the recovery kinetics and causes the channels to recover fully from inactivation. The fast and slow recovery time constants of  $\text{Na}_v1.7 + \beta_1$  are  $6.6 \pm 0.6$  msec ( $\tau_F$ ) and  $53.2 \pm 12.7$  msec ( $\tau_S$ ;  $n = 7$ ). The more complete recovery of  $\text{Na}_v1.7 + \beta_1$  channels can be attributed primarily to a 2.9-fold increase in the fraction of channels recovering with the rapid time constant.

In contrast, the recovery from fast inactivation of  $\text{Na}_v1.8$  is slow in comparison with  $\text{Na}_v1.7$ , and fitting the data required the sum of three exponentials to describe the time course accurately. The recovery time constants of  $\text{Na}_v1.8$  channels are  $9.9 \pm 1.8$  msec ( $\tau_F$ ),  $168.6 \pm 52.2$  msec ( $\tau_I$ ), and  $787.6 \pm 112.6$  msec ( $\tau_S$ ;  $n = 5$ ) (Fig. 5*D*). The recovery time constants of  $\text{Na}_v1.8 + \beta_1$  are  $2.0 \pm 0.3$  msec ( $\tau_F$ ),  $243.8 \pm 85.4$  msec ( $\tau_I$ ), and  $1070.1 \pm 59.0$  msec ( $\tau_S$ ;  $n = 4$ ) (Fig. 5*D*). The  $\beta_1$  subunit reduces  $\tau_F$  but increases  $\tau_S$ , consistent with differential effects on the fast and slow components of  $\text{Na}_v1.8$  recovery from inactivation. Interestingly, the slow component of recovery ( $\tau_S$ ) is observed only with  $\text{Na}_v1.8$  channels and is enhanced with the  $\beta_1$  subunit. This suggests that the  $\text{Na}_v1.8 + \beta_1$  channels may enter readily into a slow inactivated state during the short (40 msec) depolarizing prepulses to  $+20$  mV that are used to induce inactivation.

#### Development of slow inactivation of $\text{Na}_v1.7 + \beta_1$ and $\text{Na}_v1.8 + \beta_1$ channels

The recovery from inactivation of  $\text{Na}_v1.8 + \beta_1$  displays a slow component that is not observed with  $\text{Na}_v1.7 + \beta_1$  (Fig. 5*C,D*). The data suggest that, in addition to the fast and intermediate components of inactivation observed for both channels,  $\text{Na}_v1.8 + \beta_1$  channels enter into a slow inactivated state during the short depolarizing prepulses used to inactivate the channels in these experiments. To test this hypothesis, we compared the development of slow inactivation of  $\text{Na}_v1.7 + \beta_1$  and  $\text{Na}_v1.8 + \beta_1$  channels (Fig. 6). The onset of slow inactivation was measured by depolarizing the oocytes to either  $-20$  mV ( $\text{Na}_v1.7 + \beta_1$ ) or  $+20$  mV ( $\text{Na}_v1.8 + \beta_1$ ) for a variable interval (0 msec to 10 sec) to induce inactivation. Then the voltage was returned to  $-100$  mV for 20 msec to allow for the recovery of fast-inactivated channels ( $\tau_F = 6.6$  msec for  $\text{Na}_v1.7 + \beta_1$ ;  $\tau_F = 2$  msec for  $\text{Na}_v1.8 + \beta_1$ ) before a standard test pulse to assay availability was applied. The amplitudes of the test currents were normalized to controls and plotted versus the prepulse interval. In these experiments the progressive

**Figure 5.** Effects of the  $\beta_1$  subunit on the activation, inactivation, and recovery of  $\text{Na}_v1.7$  and  $\text{Na}_v1.8$  channels. Activation was measured by applying a series of depolarizing voltage pulses between  $-80$  and  $+60$  mV from a holding potential of  $-100$  mV. The peak currents were measured, and the relative conductance was calculated by using the standard procedures (see Materials and Methods). Also plotted is the steady-state availability curve that was determined by using 500 msec conditioning pulses to voltages between  $-110$  and  $+30$  mV and a standard test pulse to either  $-20$  mV ( $\text{Na}_v1.7$  and  $\text{Na}_v1.7+\beta_1$ ) or  $+20$  mV ( $\text{Na}_v1.8$  and  $\text{Na}_v1.8+\beta_1$ ). Test currents were normalized and plotted versus conditioning voltage. **A**, The normalized conductance versus voltage and steady-state inactivation plots of  $\text{Na}_v1.7$  (filled squares) and  $\text{Na}_v1.7+\beta_1$  (open squares) channels. The smooth curves are Boltzmann fits:  $G = 1/(1 + \exp((V - V_{0.5})/k))$ , with midpoints ( $V_{0.5}$ ) and slope factors ( $k$ ) of activation of  $-22 \pm 2.2$  and  $5.4 \pm 0.4$  mV for  $\text{Na}_v1.7$  ( $n = 10$ ) and  $-27.7 \pm 1.3$  and  $3.7 \pm 0.2$  mV for  $\text{Na}_v1.7+\beta_1$  ( $n = 11$ ). For inactivation the  $V_{0.5}$  and  $k$  values are  $-68.2 \pm 0.43$  and  $6.4 \pm 0.45$  mV for  $\text{Na}_v1.7$  ( $n = 4$ ) and  $-69.8 \pm 0.3$  and  $3.9 \pm 0.2$  mV for  $\text{Na}_v1.7+\beta_1$  ( $n = 4$ ). **B**, Steady-state activation and inactivation of  $\text{Na}_v1.8$  channels. The smooth curves have  $V_{0.5}$  and  $k$  values for activation of  $4.7 \pm 0.7$  and  $6.8 \pm 0.1$  mV for  $\text{Na}_v1.8$  (filled circles;  $n = 8$ ) and  $-3.3 \pm 1.0$  and  $5.5 \pm 0.1$  mV for  $\text{Na}_v1.8+\beta_1$  (open circles;  $n = 9$ ). The  $V_{0.5}$  and  $k$  values for inactivation are  $-54.8 \pm 1.7$  and  $8.4 \pm 0.2$  mV for  $\text{Na}_v1.8$  ( $n = 3$ ) and  $-62.6 \pm 2.3$  and  $6.3 \pm 0.7$  mV for  $\text{Na}_v1.8+\beta_1$  ( $n = 6$ ). **C**, **D**, The time course of recovery from inactivation of  $\text{Na}_v1.7$  and  $\text{Na}_v1.8$  channels. Inactivation was induced by depolarizing to  $-20$  mV ( $\text{Na}_v1.7$  and  $\text{Na}_v1.7+\beta_1$ ) or  $+20$  mV ( $\text{Na}_v1.8$  and  $\text{Na}_v1.8+\beta_1$ ) for 50 msec before returning to  $-100$  mV for intervals between 1 msec and 5 sec. A standard test pulse was used to monitor recovery, and the normalized test currents were plotted versus the recovery interval. **C**, Recovery from inactivation of  $\text{Na}_v1.7$  (filled squares) and  $\text{Na}_v1.7+\beta_1$  (open squares) channels. The smooth curves are fits to the sum of two exponentials:  $I/I_0 = A_F \cdot (1 - \exp(-t/\tau_F)) + A_S \cdot (1 - \exp(-t/\tau_S))$ , with time constants ( $\tau$ ) and weighting factors ( $A$ ) of  $19.6 \pm 0.8$  msec ( $\tau_F$ ;  $A_F = 0.46 \pm 0.02$ ) and  $933.4 \pm 54.6$  msec ( $\tau_S$ ;  $A_S = 0.54 \pm 0.02$ ) for  $\text{Na}_v1.7$  ( $n = 7$ ) and  $6.6 \pm 0.6$  msec ( $\tau_F$ ;  $A_F = 0.89 \pm 0.02$ ) and  $53.2 \pm 12.7$  msec ( $\tau_S$ ;  $A_S = 0.11 \pm 0.02$ ) for  $\text{Na}_v1.7+\beta_1$  ( $n = 7$ ). **D**, The recovery of  $\text{Na}_v1.8$  (filled circles) and  $\text{Na}_v1.8+\beta_1$  (open circles) channels is described best by the sum of three exponentials:  $I/I_0 = A_F \cdot (1 - \exp(-t/\tau_F)) + A_I \cdot (1 - \exp(-t/\tau_I)) + A_S \cdot (1 - \exp(-t/\tau_S))$ , where  $\tau_F$ ,  $\tau_I$ , and  $\tau_S$  are the fast, intermediate, and slow recovery time constants, and  $A_F$ ,  $A_I$ , and  $A_S$  are the relative weighting factors.  $t$  is the interpulse duration, and  $I/I_0$  is the normalized current amplitude. Data are the means  $\pm$  SEM. The time constants of  $\text{Na}_v1.8$  are  $9.9 \pm 1.8$  msec ( $\tau_F$ ;  $A_F = 0.41 \pm 0.04$ ),  $168.6 \pm 52.2$  msec ( $\tau_I$ ;  $A_I = 0.28 \pm 0.04$ ), and  $787.6 \pm 112.6$  msec ( $\tau_S$ ;  $A_S = 0.28 \pm 0.04$ ) (filled circles;  $n = 5$ ). Recovery time constants of  $\text{Na}_v1.8+\beta_1$  are  $2.0 \pm 0.3$  msec ( $\tau_F$ ;  $A_F = 0.32 \pm 0.05$ ),  $243.8 \pm 85.4$  msec ( $\tau_I$ ;  $A_I = 0.34 \pm 0.05$ ), and  $1070.1 \pm 59.0$  msec ( $\tau_S$ ;  $A_S = 0.34 \pm 0.02$ ) (open circles;  $n = 4$ ).



decay of the currents observed with increasing prepulse duration reflects the entry of the channels into slow inactivated states from which the channels do not recover readily during the short hyperpolarization ( $-100$  mV for 20 msec) that precedes the test pulse (Fig. 6). The onset of slow inactivation of the  $\text{Na}_v1.7+\beta_1$  channels is fit with the sum of three exponentials with time constants of  $32.6 \pm 1.5$  msec ( $\tau_F$ ),  $556.5 \pm 104.4$  msec ( $\tau_I$ ), and  $4071.9 \pm 155.1$  msec ( $\tau_S$ ;  $n = 6$ ) (Fig. 6). For  $\text{Na}_v1.8+\beta_1$  channels the onset of slow inactivation has time constants of  $8.4 \pm 0.2$  msec ( $\tau_F$ ),  $200.0 \pm 30.0$  msec ( $\tau_I$ ), and  $8880.0 \pm 1150.0$  msec ( $\tau_S$ ;  $n = 5$ ) (Fig. 6). These data indicate that the onset of slow inactivation ( $\tau_F$ ) is nearly fourfold faster for the  $\text{Na}_v1.8+\beta_1$  channels than for  $\text{Na}_v1.7+\beta_1$  channels. The rapid development of slow inactivation

of  $\text{Na}_v1.8+\beta_1$  may account for the unusually slow component of recovery from inactivation observed for this isoform. In contrast, the onset of slow inactivation of  $\text{Na}_v1.7+\beta_1$  channels is delayed in comparison with  $\text{Na}_v1.8+\beta_1$ , and these channels consequently lack the slow component of recovery from inactivation (Fig. 5C).

#### Frequency-dependent inhibition of $\text{Na}_v1.7+\beta_1$ and $\text{Na}_v1.8+\beta_1$ channels

The unusually rapid onset of slow inactivation of  $\text{Na}_v1.8+\beta_1$  suggests that during short depolarizations ( $<10$  msec) some of the channels are likely to enter into a slow inactivated state. This could have important consequences for the rapid cycling of chan-

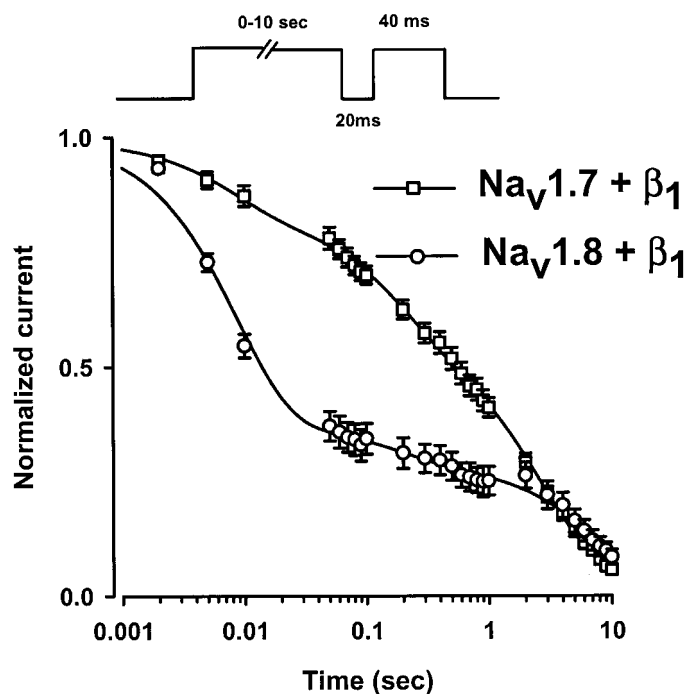


**Figure 6.** Development of slow inactivation of  $\text{Na}_v1.7+\beta_1$  and  $\text{Na}_v1.8+\beta_1$  sodium channels. Time course of entry into the slow inactivated state was measured by using a triple-pulse protocol consisting of a variable duration conditioning pulse (2 msec to 10 sec) to  $-20$  mV ( $\text{Na}_v1.7+\beta_1$ ; open squares) or to  $+20$  mV ( $\text{Na}_v1.8+\beta_1$ ; open circles) to inactivate the channels. A 20 msec pulse to  $-100$  mV was applied to promote the rapid recovery of inactivated channels, and a standard test pulse was used to assay availability. The test currents were normalized and plotted versus the conditioning pulse interval. The decay of the currents is fit best by the sum of three exponentials:  $I/I_o = A_F \cdot (1 - \exp(-t/\tau_F)) + A_I \cdot (1 - \exp(-t/\tau_I)) + A_S \cdot (1 - \exp(-t/\tau_S))$ , where  $\tau_F$ ,  $\tau_I$ , and  $\tau_S$  are the time constants, and  $A_F$ ,  $A_I$ , and  $A_S$  are the relative weighting factors.  $t$  is the conditioning pulse duration, and  $I/I_o$  is the normalized current. The data are the means  $\pm$  SEM. The time constants of  $\text{Na}_v1.7+\beta_1$  (open squares) are  $\tau_F = 32.6 \pm 1.5$  msec ( $A_F = 0.25 \pm 0.03$ ),  $\tau_I = 556.5 \pm 104.4$  msec ( $A_I = 0.33 \pm 0.02$ ), and  $\tau_S = 4071.9 \pm 155.1$  msec ( $A_S = 0.42 \pm 0.03$ ) ( $n = 6$ ). For  $\text{Na}_v1.8+\beta_1$  (open circles) the time constants are  $\tau_F = 8.4 \pm 1.5$  msec ( $A_F = 0.57 \pm 0.07$ ),  $\tau_I = 200.0 \pm 30.0$  msec ( $A_I = 0.16 \pm 0.07$ ), and  $\tau_S = 8880.0 \pm 1150.0$  msec ( $A_S = 0.27 \pm 0.04$ ) ( $n = 5$ ).

nels during episodes of repetitive stimulation. The effects of rapid pulsing were tested by applying a series of 50 short (8 msec) depolarizing pulses ( $-20$  mV for  $\text{Na}_v1.7+\beta_1$  or  $+20$  mV for  $\text{Na}_v1.8+\beta_1$ ) at frequencies of between 0.5 and 100 Hz (Fig. 7). The 8 msec depolarizing pulse used in the experiments is close to the somatic action potential duration of C fibers (0.6–7.4 msec) previously reported by Harper and Lawson (1985). The currents elicited by the individual test pulses were normalized to control currents and plotted versus the pulse number. For  $\text{Na}_v1.7+\beta_1$  channels, pulsing frequencies up to 20 Hz have small effects on the amplitude of the currents (Fig. 7A,C;  $n = 10$ ). The majority of the channels is capable of efficiently cycling via the open, closed, and inactivated conformations at these pulsing frequencies. Increasing the stimulation frequency to 50 or 100 Hz dramatically reduces the currents of  $\text{Na}_v1.7+\beta_1$ , indicating that the channels no longer fully recover during the short intervals between pulses. The decrease in amplitude for pulsing frequencies  $>25$  Hz may reflect the trapping of some channels in slow inactivated states (Fig. 5C).

The response of  $\text{Na}_v1.7+\beta_1$  channels to rapid repetitive stim-

ulation sharply contrasts with that of  $\text{Na}_v1.8+\beta_1$  channels in which the pulsing frequencies of 1–2 Hz cause a significant reduction in current amplitude (Fig. 7B,C;  $n = 8$ ). At frequencies  $>20$  Hz the current amplitude reaches a steady-state level of  $\sim 42\%$  of the control current (Fig. 7B,C). The dissimilarity of  $\text{Na}_v1.8+\beta_1$  and  $\text{Na}_v1.7+\beta_1$  channels in their sensitivity to rapid repetitive stimulation could have important consequences on the firing frequency of cells predominantly expressing these types of sodium channels.

## DISCUSSION

Despite a high degree of sequence homology, the  $\alpha$  subunits of voltage-gated sodium channels exhibit substantial heterogeneity in their electrophysiological properties (Goldin et al., 2000). Subtle changes in the primary amino acid sequences can have significant effects in the gating and pharmacology of these channels. In addition to the functional differences encoded in the  $\alpha$  subunits, most sodium channels are multimeric proteins that are associated with accessory  $\beta$  subunits ( $\beta_1$ ,  $\beta_2$ , and  $\beta_3$ ) (Isom et al., 1992; McClatchey et al., 1993; Nuss et al., 1995). The  $\beta_1$  subunit is known to accelerate the kinetics of activation, inactivation, and recovery from inactivation of brain and skeletal muscle sodium channels (Auld et al., 1988). Modulation of these channels by the  $\beta_1$  subunit also contributes to the functional diversity of neuronal and muscle sodium channels.

In this study we examined the effects of the  $\beta_1$  subunit on the functional properties of the  $\text{Na}_v1.7$  (PN1) and  $\text{Na}_v1.8$  (PN3) sodium channels heterologously expressed in *Xenopus* oocytes. Our data indicate that the  $\beta_1$  subunit alters the gating and voltage sensitivity of both channels and selectively increases the expression of the  $\text{Na}_v1.8$  channels.

### The $\beta_1$ subunit modulates levels of sodium currents of $\text{Na}_v1.7$ and $\text{Na}_v1.8$

The  $\beta_1$  subunit selectively enhances the expression of  $\text{Na}_v1.8$  channels, but not  $\text{Na}_v1.7$  channels (Fig. 2). Comparing the average sodium current from paired groups of oocytes indicates that the expression of  $\text{Na}_v1.8$  increases by almost sixfold in the presence of the  $\beta_1$  subunit versus 1.1-fold for  $\text{Na}_v1.7$ . The selective regulation of  $\text{Na}_v1.8$  sodium channel expression by the  $\beta_1$  subunit may play an important role in regulating TTX-R current *in vivo* (Cummins and Waxman, 1997; Novakovic et al., 1998; Gold, 1999). A similar modulation of  $\text{Na}_v1.8$  sodium channel expression was observed recently with another auxiliary ( $\beta_3$ ) subunit (Shah et al., 2000).

### The $\beta_1$ subunit alters gating and voltage sensitivity of $\text{Na}_v1.7$ and $\text{Na}_v1.8$ sodium channels

Coexpression with the  $\beta_1$  subunit significantly alters the kinetics and voltage sensitivity of  $\text{Na}_v1.7$  and  $\text{Na}_v1.8$  sodium currents. In the absence of  $\beta_1$  the inactivation of  $\text{Na}_v1.7$  is slow and incomplete. The  $\beta_1$  subunit accelerates the current decay consistent with a more rapid rate of inactivation. At  $-20$  mV the inactivation of  $\text{Na}_v1.7$  increases nearly 10-fold when the channels are coexpressed with the  $\beta_1$  subunit. The  $\beta_1$  subunit also alters the voltage sensitivity of the channels, shifting the midpoints of steady-state activation and inactivation by  $-5.3$  and  $-1.6$  mV, respectively.

Similar changes in current kinetics and voltage sensitivity are observed when the  $\text{Na}_v1.8$  channels are coexpressed with the  $\beta_1$  subunit. Coexpression with the  $\beta_1$  subunit decreases the time constant of current decay at  $+20$  mV by 1.6-fold, consistent with more rapid inactivation. In the presence of the  $\beta_1$  subunit the

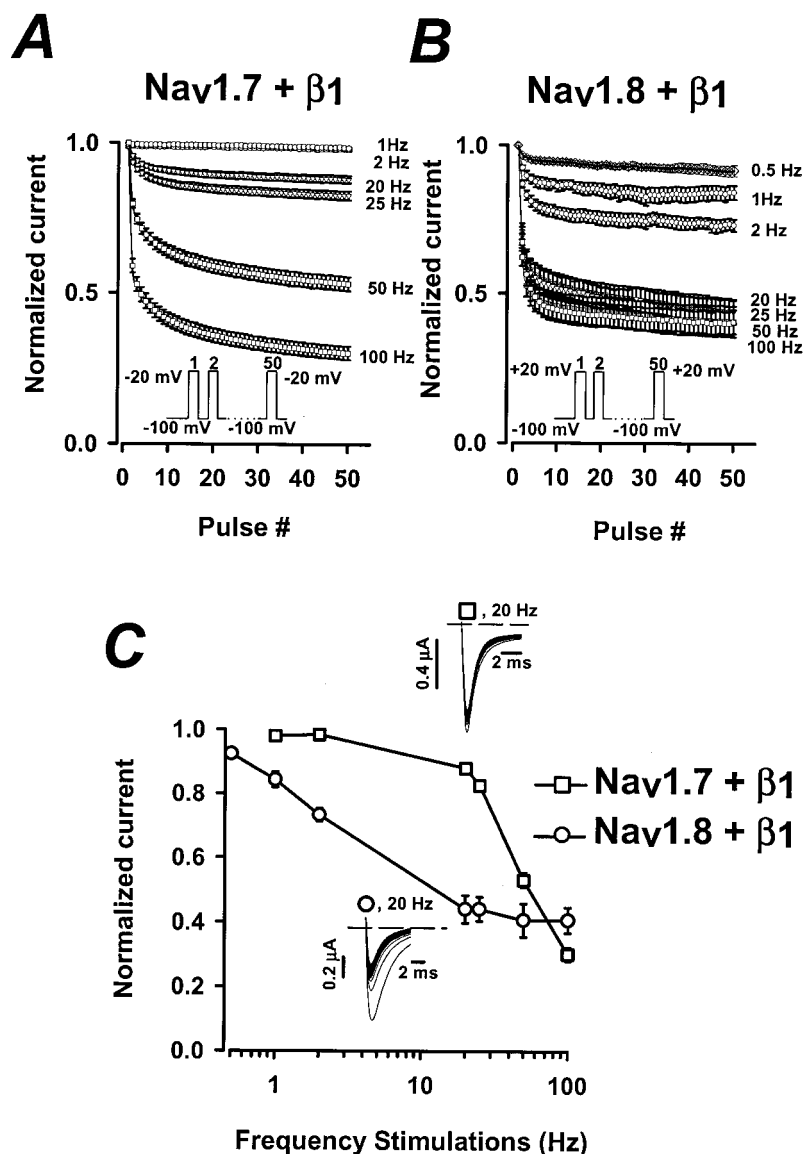


**Figure 7.** Frequency-dependent inhibition of  $\text{Na}_v1.7+\beta_1$  and  $\text{Na}_v1.8+\beta_1$  sodium currents. *A, B*, A train of 50 pulses was applied to  $-20$  mV ( $\text{Na}_v1.7+\beta_1$ ;  $n = 11$ ) or  $+20$  mV ( $\text{Na}_v1.8+\beta_1$ ;  $n = 8$ ) at frequencies between 0.5 and 100 Hz. The peak currents elicited by each test pulse were normalized to the current of the first pulse ( $P_n/P_1$ , where  $n = 1-50$ ) and were plotted versus pulse number. The pulse duration was 8 msec for frequencies between 0.5 and 50 Hz but was reduced to 5 msec for the 100 Hz experiments. The holding and interpulse potential was  $-100$  mV. *C*, Plotted is the ratio of the currents elicited by the 50th and first pulses ( $P_{50}/P_1$ ) versus the pulsing frequency. *Insets* are representative raw current traces of  $\text{Na}_v1.7+\beta_1$  (open squares) and  $\text{Na}_v1.8+\beta_1$  (open circles) stimulated at 20 Hz.

midpoints of steady-state activation and inactivation of  $\text{Na}_v1.8$  channels are shifted significantly by  $-8$  and  $-7.8$  mV, respectively.

### The $\beta_1$ subunit alters the recovery from fast inactivation

The  $\beta_1$  subunit also significantly affects the time course of recovery from inactivation of the  $\text{Na}_v1.7$  and  $\text{Na}_v1.8$  sodium channels (Fig. 5*C,D*). The recovery from inactivation of  $\text{Na}_v1.7$  is well fit by two exponentials with time constants of 19 and 933 msec for  $\text{Na}_v1.7$  and time constants of 6.6 and 53 msec for  $\text{Na}_v1.7+\beta_1$ . The recovery of the  $\text{Na}_v1.8$  channels is also considerably slower and requires three exponentials to describe the time course adequately. Coexpression of  $\text{Na}_v1.8$  with the  $\beta_1$  subunit accelerates the fast component of recovery from inactivation but delays the intermediate and slow components of recovery from fast inactivation. The mechanism underlying this differential effect on the fast and slow components of inactivation is currently under investigation.

Our data indicate that the  $\beta_1$  subunit has significant effects on both the  $\text{Na}_v1.7$  and  $\text{Na}_v1.8$  channels, particularly on the kinetics of inactivation. A similar increase in inactivation rate with  $\beta_1$  coexpression recently has been reported for  $\text{Na}_v1.7$  channels

(Shcherbatko et al., 1999). These findings are inconsistent with previous studies showing that the functional properties of  $\text{Na}_v1.7$  and  $\text{Na}_v1.8$  channels expressed in oocytes are not altered by the  $\beta_1$  subunit (Sangameswaran et al., 1996, 1997). Although we have no clear explanation for the differences between our data and those of these previous investigators, our data are consistent with studies showing that the  $\beta_1$  subunit modulates the gating and expression of many neuronal sodium channels (Isom et al., 1995; Shcherbatko et al., 1999).

### Comparison with TTX-S and TTX-R sodium channels of DRG neurons

Multiple components of sodium current have been recorded from native DRG neurons that exhibit significant differences in gating and toxin sensitivity (Kostyuk et al., 1981; Roy and Narahashi, 1992; Ogata and Tatebayashi, 1993; Rush et al., 1998). The kinetics of the TTX-S currents are generally faster, and the steady-state activation and inactivation are shifted toward more hyperpolarized voltages in comparison with the TTX-R currents. These properties are qualitatively consistent with those of the  $\text{Na}_v1.7$  (TTX-S) and  $\text{Na}_v1.8$  (TTX-R) sodium channels observed

in this study. For the  $\text{Na}_v1.7+\beta_1$  channels the midpoints of steady-state activation, inactivation, and the kinetics of inactivation are in reasonable agreement with the properties of TTX-S currents measured from acutely dissociated DRG neurons (Kostyuk et al., 1981; Roy and Narahashi, 1992; Ogata and Tatebayashi, 1993; Rush et al., 1998). The  $\text{Na}_v1.7$  channel, along with its associated  $\beta_1$  subunit, is likely to contribute to TTX-S sodium currents of both large and small DRG neurons (Ogata and Tatebayashi, 1993; Rush et al., 1998).

In contrast, the midpoint steady-state inactivation of  $\text{Na}_v1.8+\beta_1$  ( $-62.6$  mV) is more hyperpolarized than the native TTX-R sodium currents ( $-34$  to  $-52$  mV). The reasons for this discrepancy are unclear; however, a recent study has shown that at least three distinct components of TTX-R sodium current are present in the native cells (Rush et al., 1998). Variation in the relative expression levels of these different TTX-R sodium channels may explain the wide range of electrophysiological properties reported for the TTX-R currents of DRG neurons. In addition, the presence of additional  $\beta$  subunits ( $\beta_2$ ,  $\beta_3$ ) or a variation in second messenger regulation may contribute further to the differences in the inactivation of heterologously expressed  $\text{Na}_v1.8$  and the TTX-R current of DRG neurons. In addition, our data show that the development of slow inactivation of the  $\text{Na}_v1.8+\beta_1$  channels is unusually rapid. This can influence the properties of steady-state inactivation by shifting the midpoint toward more hyperpolarized voltages (Ogata and Tatebayashi, 1992). Interestingly, a TTX-R3 component of sodium current of type D DRG neurons has been identified recently that has a midpoint of steady-state inactivation of  $-63$  mV, identical to what we observed for the  $\text{Na}_v1.8+\beta_1$  channels (Rush et al., 1998). Despite some quantitative differences the data indicate that coexpression of  $\text{Na}_v1.8$  and the  $\beta_1$  subunits in oocytes produces currents that have kinetics and voltage sensitivity similar to the TTX-R sodium currents of small DRG neurons.

Several studies have shown that the amplitudes of DRG neuron sodium currents are highly sensitive to the frequency of the applied voltage pulses (Rush et al., 1998; Scholz et al., 1998). In general, the TTX-R currents are reported to be more sensitive to rapid repetitive pulsing than the TTX-S sodium currents. These data suggest important differences in the repriming of these channels after a depolarizing voltage pulse. In this study the  $\text{Na}_v1.8+\beta_1$  channels display a significant reduction in current amplitude during repetitive stimulation at frequencies between 1 and 2 Hz (Fig. 7). This contrasts with  $\text{Na}_v1.7+\beta_1$  channels, which are considerably less sensitive to such low-frequency stimulation. The data suggest that during low-frequency repetitive stimulation (1–2 Hz) inactivated  $\text{Na}_v1.8+\beta_1$  channels fail to recover fully during the interval between pulses. At 2 Hz the rest interval between pulses (492 msec) is sufficient to permit full recovery of fast inactivated channels ( $\tau_F = 2$  msec). The entry and recovery from fast inactivation cannot account for the observed frequency-dependent reduction of  $\text{Na}_v1.8+\beta_1$  currents. Rather, the data suggest that a fraction of  $\text{Na}_v1.8+\beta_1$  channels may enter into a slow inactivated state during the brief depolarizations. The time course of entry into the slow inactivated state has been measured directly by a double-pulse protocol (Fig. 6). The onset of slow inactivation of  $\text{Na}_v1.8+\beta_1$  channels ( $\tau_F = 8.4$  msec) is considerably faster than that of the  $\text{Na}_v1.7+\beta_1$  channels ( $\tau_F = 33$  msec). During the short depolarizations used in the repetitive pulsing protocol (8 msec), a significant fraction of the  $\text{Na}_v1.8+\beta_1$  channels, but not  $\text{Na}_v1.7+\beta_1$  channels, is predicted to undergo slow inactivation. Few of these slow inactivated channels recover ( $\tau_S =$

1070 msec) during the short interval (492 msec) between pulses. The data indicate that the high sensitivity of the  $\text{Na}_v1.8+\beta_1$  channels to low-frequency repetitive stimulation results from the unusually rapid entry of these channels into the slow inactivated state. A similar mechanism has been proposed for the TTX-R sodium current of DRG neurons (Scholz et al., 1998).  $\text{Na}_v1.7+\beta_1$  channels are more resistant to slow inactivation and are significantly less sensitive to low-frequency repetitive stimulation.

### Physiological relevance

Previous work suggests that the rapid repriming and high threshold of TTX-R sodium currents may play an important role in the sustained firing of C fibers after nerve injury (Elliott and Elliott, 1993; Jęftinija, 1994; Schild and Kunze, 1997). Although the majority of the  $\text{Na}_v1.8+\beta_1$  channels rapidly recovers from inactivation, these channels are also more likely to entering slow inactivated states. During sustained repetitive firing a significant fraction of the  $\text{Na}_v1.8+\beta_1$  channels is likely to accumulate in this slow inactivated state. However, at very high frequencies ( $>20$  Hz) the amplitudes of  $\text{Na}_v1.8+\beta_1$  currents reach steady state, being reduced 58% in comparison with the initial current level (Fig. 7). This is nearly equivalent to the fraction of channels (58.3%) that rapidly enters into the slow repriming state in response to sustained depolarization ( $\tau_F = 8$  msec) (Fig. 7). The data suggest that during repetitive pulsing at high frequency ( $>20$  Hz), or in response to sustained depolarization, 60% of the  $\text{Na}_v1.8+\beta_1$  channels rapidly enter into slow inactivated states; however, the other 40% of active channels will contribute to action potential firing.

In addition, the atypical kinetics and voltage sensitivity of the  $\text{Na}_v1.8+\beta_1$  sodium channels may contribute to the unusual electrical excitability of the small nociceptive neurons in which these channels are expressed preferentially (Caffrey et al., 1992; Arbuckle and Docherty, 1995; Novakovic et al., 1998). The relative contribution of the  $\text{Na}_v1.8+\beta_1$  channels to the total sodium current of nociceptive neurons may contribute to the high threshold (McLean et al., 1988) and slow firing frequency of C fibers (Harper and Lawson, 1985). The slow inactivation and recovery kinetics of the  $\text{Na}_v1.8+\beta_1$  channels would tend to broaden the action potential and reduce the firing frequency of these neurons. These unique properties of the  $\text{Na}_v1.8+\beta_1$  channels may play a role in the adaptation of nociceptive nerve impulses during low firing frequency. On the other hand, the resistance of  $\text{Na}_v1.8+\beta_1$  channels to enter fully into the slow inactivated state during high-frequency ( $>20$  Hz) stimulation, coupled with the high threshold for activation ( $V_{0.5} = -3.3$  mV), could maintain a minimal level of sodium channel activity in rapidly firing or chronically depolarized neurons during sustain noxious stimuli. This may enable pain fibers to continue generating action potentials after peripheral nerve damage.

In conclusion, the present study shows that the modulatory effects of the  $\beta_1$  subunit are likely to have important consequences for the electrical excitability of the DRG neurons expressing these channels. However, the existence of other auxiliary subunits ( $\beta_2$  and  $\beta_3$ ) in these nociceptive C fibers (Shah et al., 2000; Coward et al., 2001) could have complementary regulatory effects on  $\text{Na}_v1.7+\beta_1$  and  $\text{Na}_v1.8+\beta_1$  function. The possible roles of the other  $\beta$  subunits need to be tested.

### REFERENCES

- Akopian AN, Sivillotti L, Wood JN (1996) A tetrodotoxin-resistant voltage-gated sodium channel expressed by sensory neurons. *Nature* 379:257–262.

- Arbuckle JB, Docherty RJ (1995) Expression of tetrodotoxin-resistant sodium channels in capsaicin-sensitive dorsal root ganglion neurons of adult rats. *Neurosci Lett* 185:70–73.
- Auld VJ, Goldin AL, Krafte DS, Marshall J, Dunn JM, Catterall WA, Lester HA, Davidson N, Dunn RJ (1988) A rat brain  $\text{Na}^+$  channel  $\alpha$  subunit with novel gating properties. *Neuron* 1:449–461.
- Bennett Jr PB, Makita N, George Jr AL (1993) A molecular basis for gating mode transitions in human skeletal muscle  $\text{Na}^+$  channels. *FEBS Lett* 326:21–24.
- Black JA, Dib-Hajj S, McNabola K, Jeste S, Rizzo MA, Kocsis JD, Waxman SG (1996) Spinal sensory neurons express multiple sodium channel  $\alpha$  subunit mRNAs. *Brain Res Mol Brain Res* 43:117–131.
- Blackburn-Munro G, Fleetwood-Walker SM (1999) The sodium channel auxiliary subunits  $\beta_1$  and  $\beta_2$  are differentially expressed in the spinal cord of neuropathic rats. *Neuroscience* 90:153–164.
- Caffrey JM, Eng DL, Black JA, Waxman SG, Kocsis JD (1992) Three types of sodium channels in adult rat dorsal root ganglion neurons. *Brain Res* 592:283–297.
- Caldwell JH (2000) Clustering of sodium channels at the neuromuscular junction. *Microsc Res Tech* 49:84–89.
- Chahine M, Bennett PB, George Jr AL, Horn R (1994) Functional expression and properties of the human skeletal muscle sodium channel. *Pflügers Arch* 427:136–142.
- Coward K, Jowett A, Plumpton S, Powell A, Birch R, Tate S, Bountra C, Anand P (2001) Sodium channel  $\beta_1$  and  $\beta_2$  subunits parallel SNS/PN3  $\alpha$  subunit changes in injured human sensory neurons. *NeuroReport* 12:483–488.
- Cummins TR, Waxman SG (1997) Downregulation of tetrodotoxin-resistant sodium currents and upregulation of a rapidly repriming tetrodotoxin-sensitive sodium current in small spinal sensory neurons after nerve injury. *J Neurosci* 17:3503–3514.
- Dib-Hajj SD, Tyrrell L, Black JA, Waxman SG (1998)  $\text{NaN}$ , a novel voltage-gated  $\text{Na}$  channel, is expressed preferentially in peripheral sensory neurons and down-regulated after axotomy. *Proc Natl Acad Sci USA* 95:8963–8968.
- Elliott AA, Elliott JR (1993) Characterization of TTX-sensitive and TTX-resistant sodium currents in small cells from adult rat dorsal root ganglia. *J Physiol (Lond)* 463:39–56.
- Gold MS (1999) Tetrodotoxin-resistant  $\text{Na}^+$  currents and inflammatory hyperalgesia. *Proc Natl Acad Sci USA* 96:7645–7649.
- Gold MS, Reichling DB, Shuster MJ, Levine JD (1996) Hyperalgesic agents increase a tetrodotoxin-resistant  $\text{Na}^+$  current in nociceptors. *Proc Natl Acad Sci USA* 93:1108–1112.
- Goldin AL, Snutch T, Lübbert H, Dowsett A, Marshall J, Auld V, Downey W, Fritz LC, Lester HA, Dunn R, Catterall WA, Davidson N (1986) Messenger RNA coding for only the  $\alpha$  subunit of the rat brain  $\text{Na}$  channel is sufficient for expression of functional channels in *Xenopus* oocytes. *Proc Natl Acad Sci USA* 83:7503–7507.
- Goldin AL, Barchi RL, Caldwell JH, Hofmann F, Howe JR, Hunter JC, Kallen RG, Mandel G, Meisler MH, Berwald-Netter Y, Noda M, Tamkun MM, Waxman SG, Wood JN, Catterall WA (2000) Nomenclature of voltage-gated sodium channels. *Neuron* 28:365–368.
- Harper AA, Lawson SN (1985) Electrical properties of rat dorsal root ganglion neurones with different peripheral nerve conduction velocities. *J Physiol (Lond)* 359:47–63.
- Isom LL, De Jongh KS, Patton DE, Reber BF, Offord J, Charbonneau H, Walsh K, Goldin AL, Catterall WA (1992) Primary structure and functional expression of the  $\beta_1$  subunit of the rat brain sodium channel. *Science* 256:839–842.
- Isom LL, Scheuer T, Brownstein AB, Ragsdale DS, Murphy BJ, Catterall WA (1995) Functional coexpression of the  $\beta_1$  and type IIA  $\alpha$  subunits of sodium channels in a mammalian cell line. *J Biol Chem* 270:3306–3312.
- Jeftinija S (1994) The role of tetrodotoxin-resistant sodium channels of small primary afferent fibers. *Brain Res* 639:125–134.
- Kostyuk PG, Veselovsky NS, Tsyndrenko AY (1981) Ionic currents in the somatic membrane of rat dorsal root ganglion neurons. I. Sodium currents. *Neuroscience* 6:2423–2430.
- Makielski JC, Limberis JT, Chang SY, Fan Z, Kyle JW (1996) Coexpression of  $\beta_1$  with cardiac sodium channel  $\alpha$  subunits in oocytes decreases lidocaine block. *Mol Pharmacol* 49:30–39.
- Makita N, Bennett Jr PB, George Jr AL (1994) Voltage-gated  $\text{Na}^+$  channel  $\beta_1$  subunit mRNA expressed in adult human skeletal muscle, heart, and brain is encoded by a single gene. *J Biol Chem* 269:7571–7578.
- McClatchey AI, Cannon SC, Slaugenhaupt SA, Gusella JF (1993) The cloning and expression of a sodium channel  $\beta_1$  subunit cDNA from human brain. *Hum Mol Genet* 2:745–749.
- McLean MJ, Bennett PB, Thomas RM (1988) Subtypes of dorsal root ganglion neurons based on different inward currents as measured by whole-cell voltage clamp. *Mol Cell Biochem* 80:95–107.
- Morgan K, Stevens EB, Shah B, Cox PJ, Dixon AK, Lee K, Pinnock RD, Hughes J, Richardson PJ, Mizuguchi K, Jackson AP (2000) Beta 3: an additional auxiliary subunit of the voltage-sensitive sodium channel that modulates channel gating with distinct kinetics. *Proc Natl Acad Sci USA* 97:2308–2313.
- Novakovic SD, Tzoumaka E, McGivern JG, Haraguchi M, Sangameswaran L, Gogas KR, Eglén RM, Hunter JC (1998) Distribution of the tetrodotoxin-resistant sodium channel PN3 in rat sensory neurons in normal and neuropathic conditions. *J Neurosci* 18:2174–2187.
- Nuss HB, Chiamvimonvat N, Pérez-García MT, Tomaselli GF, Marbán E (1995) Functional association of the  $\beta_1$  subunit with human cardiac (hH1) and rat skeletal muscle ( $\mu 1$ ) sodium channel  $\alpha$  subunits expressed in *Xenopus* oocytes. *J Gen Physiol* 106:1171–1191.
- Ogata N, Tatebayashi H (1992) Slow inactivation of tetrodotoxin-insensitive  $\text{Na}^+$  channels in neurons of rat dorsal root ganglia. *J Membr Biol* 129:71–80.
- Ogata N, Tatebayashi H (1993) Kinetic analysis of two types of  $\text{Na}^+$  channels in rat dorsal root ganglia. *J Physiol (Lond)* 466:9–37.
- Oh Y, Sashihara S, Black JA, Waxman SG (1995)  $\text{Na}^+$  channel  $\beta_1$  subunit mRNA: differential expression in rat spinal sensory neurons. *Brain Res Mol Brain Res* 30:357–361.
- O'Leary ME (1998) Characterization of the isoform-specific differences in the gating of neuronal and muscle sodium channels. *Can J Physiol Pharmacol* 76:1041–1050.
- Porreca F, Lai J, Bian D, Wegert S, Ossipov MH, Eglén RM, Kassotakis L, Novakovic S, Rabert DK, Sangameswaran L, Hunter JC (1999) A comparison of the potential role of the tetrodotoxin-insensitive sodium channels, PN3/SNS and  $\text{NaN}/\text{SNS2}$ , in rat models of chronic pain. *Proc Natl Acad Sci USA* 96:7640–7644.
- Rizzo MA, Kocsis JD, Waxman SG (1995) Selective loss of slow and enhancement of fast  $\text{Na}^+$  currents in cutaneous afferent dorsal root ganglion neurones following axotomy. *Neurobiol Dis* 2:87–96.
- Roy ML, Narahashi T (1992) Differential properties of tetrodotoxin-sensitive and tetrodotoxin-resistant sodium channels in rat dorsal root ganglion neurons. *J Neurosci* 12:2104–2111.
- Rush AM, Bräu ME, Elliott AA, Elliott JR (1998) Electrophysiological properties of sodium current subtypes in small cells from adult rat dorsal root ganglia. *J Physiol (Lond)* 511:771–789.
- Sangameswaran L, Delgado SG, Fish LM, Koch BD, Jakeman LB, Stewart GR, Sze P, Hunter JC, Eglén RM, Herman RC (1996) Structure and function of a novel voltage-gated, tetrodotoxin-resistant sodium channel specific to sensory neurons. *J Biol Chem* 271:5953–5956.
- Sangameswaran L, Fish LM, Koch BD, Rabert DK, Delgado SG, Ilnicka M, Jakeman LB, Novakovic S, Wong K, Sze P, Tzoumaka E, Stewart GR, Herman RC, Chan H, Eglén RM, Hunter JC (1997) A novel tetrodotoxin-sensitive, voltage-gated sodium channel expressed in rat and human dorsal root ganglia. *J Biol Chem* 272:14805–14809.
- Schild JH, Kunze DL (1997) Experimental and modeling study of  $\text{Na}^+$  current heterogeneity in rat nodose neurons and its impact on neuronal discharge. *J Neurophysiol* 78:3198–3209.
- Scholz A, Kuboyama N, Hempelmann G, Vogel W (1998) Complex blockades of TTX-resistant  $\text{Na}^+$  currents by lidocaine and bupivacaine reduce firing frequency in DRG neurons. *J Neurophysiol* 79:1746–1754.
- Shah BS, Stevens EB, Gonzalez MI, Bramwell S, Pinnock RD, Lee K, Dixon AK (2000) Beta 3, a novel auxiliary subunit for the voltage-gated sodium channel, is expressed preferentially in sensory neurons and is upregulated in the chronic constriction injury model of neuropathic pain. *Eur J Neurosci* 12:3985–3990.
- Shcherbatko A, Ono F, Mandel G, Brehm P (1999) Voltage-dependent sodium channel function is regulated through membrane mechanics. *Biophys J* 77:1945–1959.
- Toledo-Aral JJ, Moss BL, He Z-J, Koszowski AG, Whisenand T, Levinson SR, Wolf JJ, Silos-Santiago I, Haleboua S, Mandel G (1997) Identification of PN1, a predominant voltage-dependent sodium channel expressed principally in peripheral neurons. *Proc Natl Acad Sci USA* 94:1527–1532.
- Wallner M, Weigl L, Meera P, Lotan I (1993) Modulation of the skeletal muscle sodium channel  $\alpha$  subunit by the  $\beta_1$  subunit. *FEBS Lett* 336:535–539.
- Yang JS, Bennett PB, Makita N, George Jr AL, Barchi RL (1993) Expression of the sodium channel  $\beta_1$  subunit in rat skeletal muscle is selectively associated with the tetrodotoxin-sensitive  $\alpha$  subunit isoform. *Neuron* 11:915–922.